3.2 Failure patterns in compression test

Fig. 5 shows the specimens after compression loading. In all specimens, cover concrete falling off, pipe buckling and damaged core concrete were observed. The specimens with 4 pipes tend to show cracks in the diagonal direction and the specimens with 8 pipes tend to show cracks in parallel to the pipes. In addition, transverse cracks in some pipes with ϕ-22mm diameter were observed due to buckling. No significant tendency in failure progress was found out by elapsed time.

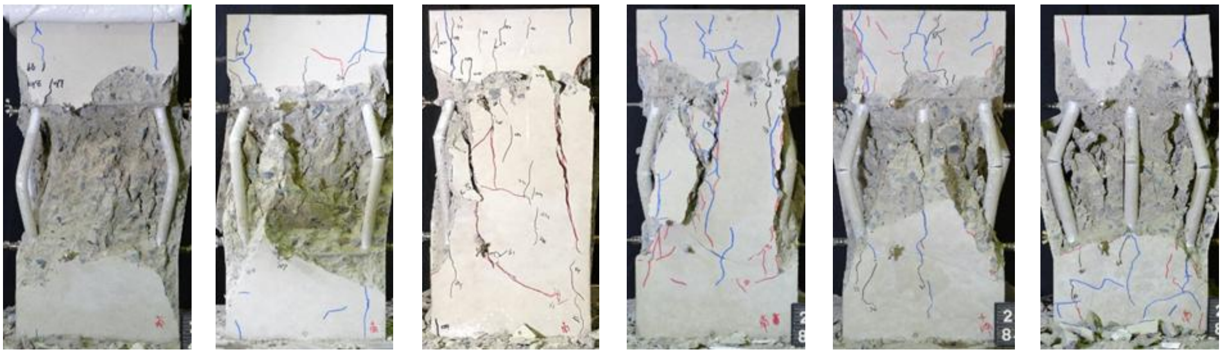

P18-N4-T15 P18-N4-T65 P18-N4-T300 P22-N8-T15 P22-N8-T65 P22-N8-T300

Fig. 5 Examples of specimens after loading

3.3 Relationship between maximum stress and crack width before loading

Table 4 showed maximum stress and strain at maximum stress. Fig. 6 shows the relationship between maximum stress and crack width before loading. Stress was calculated by dividing compressive load by cross-sectional area (250mm x 250mm), and strain was calculated by dividing axial deformation by the length of test region. There is no significant relationship between maximum stress and crack width before loading. The maximum stress of specimens with ϕ-22mm pipes is larger than that of ϕ-18mm pipes. It is considered that the maximum stress is mainly affected by the compressive capacity of the pipes.

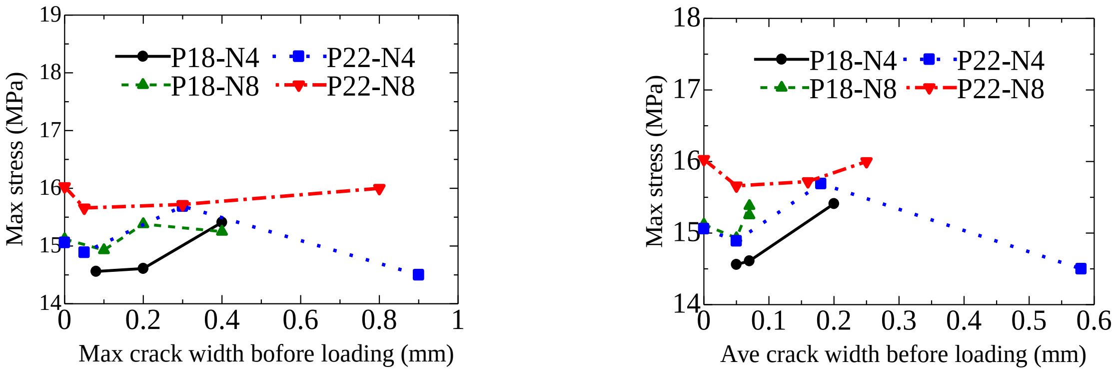

Fig. 6 Crack width before loading vs. maximum stress

3.4 Stress-strain curve

Fig. 7 shows the stress-strain curves, and Fig. 8 shows standardized stress-strain curves. Standardized stress-strain curve was calculated to focus on the softening curves after maximum stress. The larger elapsed time generally causes the softening curve gentler except for specimens of P18-N4 series.

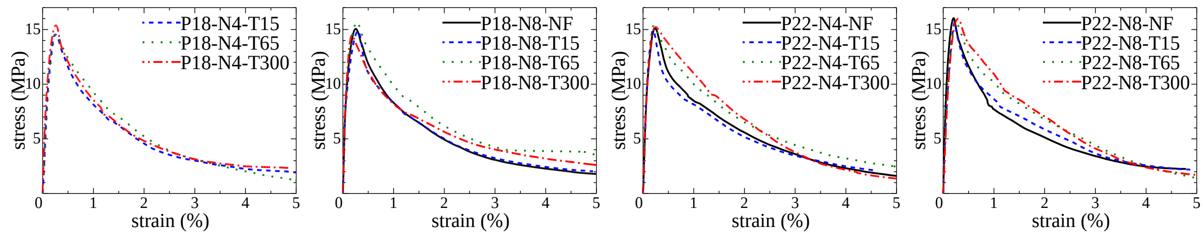

Fig. 7 Stress-strain curve

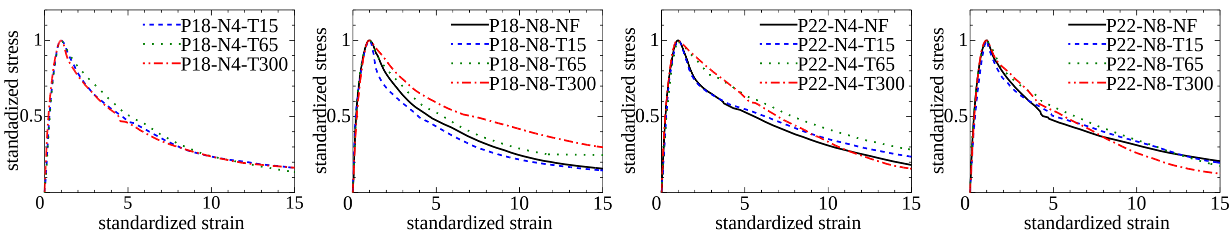

Fig. 8 Standardized stress-strain curve

4. EVALUATION OF SOFTENING GRADIENT OF CONCRETE

4.1 Calculation method of softening gradient

To calculate the softening gradient of concrete, concrete stress is obtained by substituting the stress carried by pipes from the total compressive load based on the assumption that plain section remains plain. The stress-strain curve of concrete is fitted by Popovics model (Popovics 1973) shown in Eq. (1) by the least square method using standardized stress-strain curve. The coefficient *n* in Popovics model expresses softening gradient.

$$\frac{\sigma}{\sigma_c} = \frac{n(\varepsilon/\varepsilon_c)}{n-1+(\varepsilon/\varepsilon_c)^n} \quad (1)$$

σ_c: maximum stress (MPa), ε_c: strain at maximum stress, n: coefficient

4.2 Compressive stress-strain model of pipe filled with expansion agent

The previous study (Syll 2018) reported compressive test results of pipes filled with expansion agent. These pipes have same diameter and thickness applied in this study. Furthermore, elapsed time from filling expansion agent to loading are same with that in this study. The pipe filled with expansion agent are modeled assuming that the pipes similarly behaves even in concrete. Fig. 9 shows the compressive stress-strain curve of pipes filled with expansion agent. Up to maximum, the curve is modeled by the parabola shown in Eq. (2), and the softening branch is modeled by the straight line shown in Eq. (3). The maximum stress and the strain at the maximum stress were obtained as the average value of test results of 3 specimens. The slope of the softening line of each specimen was obtained by the least square method. Table 5 shows the coefficient *m* that express the slope of softening and Fig. 9 also includes the models.

$$\sigma_p = \sigma_{max}\{2\,\varepsilon/\varepsilon_{max} - (\varepsilon/\varepsilon_{max})^2\} \tag{2}$$

$$\sigma_p = \sigma_{max}\left(1 - \frac{\varepsilon - \varepsilon_{max}}{2m\,\varepsilon_{max}}\right) \tag{3}$$

σ_{max} : maximum stress (MPa), ε_{max} : strain at maximum stress *m*: coefficient

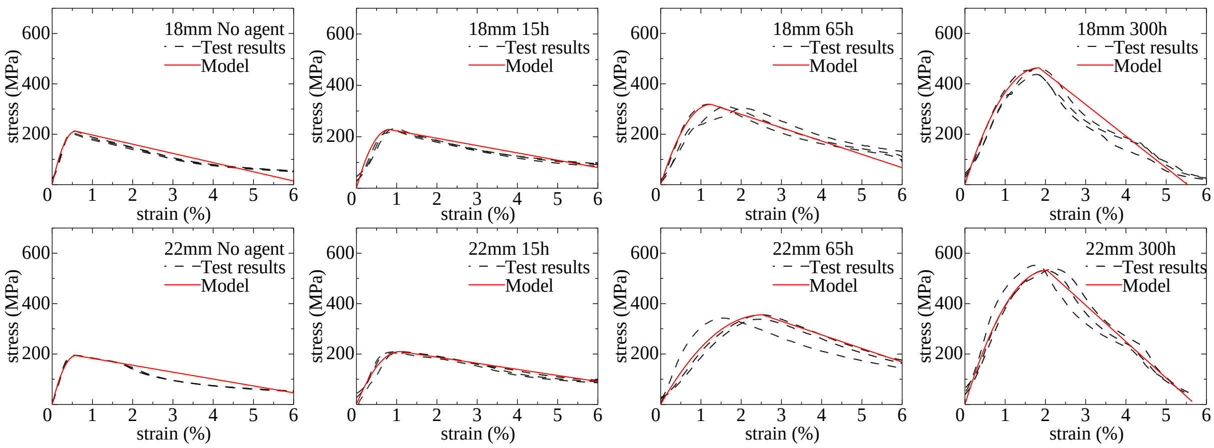

Fig. 9 Stress-strain curve of pipes filled with expansion agent

Table 5 Compressive model of pipes filled with expansion agent

Outer diameter	Elapsed time (h)	*m*	Outer diameter	Elapsed time (h)	*m*
18mm	No agent	5.0	22mm	No agent	6.0
	15	4.9		15	4.0
	65	2.4		65	1.3
	300	1.0		300	0.9

4.3 Softening gradient of concrete

Table 6 shows the maximum stress of concrete and evaluated values for *n*. Maximum stress has no significant relationship with crack width before loading as similar with that shown in Fig. 6. Fig.10 shows the examples of standardized stress-strain curve of concrete comparing fitted models. The previous study (Mogawa 2016) reported that the range of *n* was 1.75~3.48. Except for the specimens of P18-T300 series, it is recognized that the number of pipes increases, the value of *n* also increases, i.e., softening gradient tends to be large. There is no significant influence on the value of *n* by outer diameter and elapsed time. Fig. 11 shows the relationships between *n* and maximum crack width and average crack width before loading. Focusing on the specimens of P22-N8 series, the larger crack width brings the larger *n*. However, in other specimens, no relationship is observed. Table 7 shows the list of *n* and crack length ratio that proposed in the previous study (Mogawa 2016). Crack length ratio is defined as the total crack length divided by the test region length. The relationship between the crack length ratio and *n* has been evaluated by Eq. (4). In this study, cracks with a half or more of test region length are assumed to be those took place in the entire test region. The calculated values of *n* by Eq. (4) do not agree with experimental values, and the errors are large.

$$n = \frac{0.13(L_{cr}/L)+1.81}{(L_f/L)^{0.84}} \tag{4}$$

n: coefficient, L_{cr}: crack length (mm), L: test length (mm), L_f: length of local failure of concrete (mm), in this study, it is assumed that there is no local failure (L_f/L=1).

A 0.5mm thick polypropylene sheet was used to simulate crack in the previous study in which Eq. (4) was derived. Therefore, it is assumed that cracks with a width of less than 0.3mm have no effect in this study. Table 7 lists the errors between the calculation results and experimental value. The calculated results using the cracks equal or more than 0.3mm wide show smaller errors.

Table 6 List of maximum stress of concrete and evaluated values for *n*

ϕ-18mm	Max. stress (MPa)	*n*	ϕ-22mm	Max. stress (MPa)	*n*
-	-	-	P22-N4-NF	14.17	1.87
P18-N4-T15	14.20	1.99	P22-N4-T15	14.05	1.89
P18-N4-T65	14.49	1.90	P22-N4-T65	14.95	1.80
P18-N4-T300	15.04	2.02	P22-N4-T300	14.02	1.84
P18-N8-NF	14.66	1.93	P22-N8-NF	15.23	1.93
P18-N8-T15	14.71	2.13	P22-N8-T15	15.13	2.03
P18-N8-T65	15.21	1.91	P22-N8-T65	15.28	2.00
P18-N8-T300	14.82	1.87	P22-N8-T300	14.96	2.23

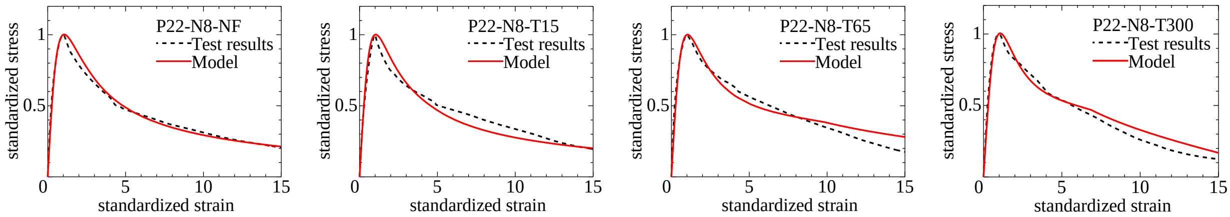

Fig. 10 Example of fitted model

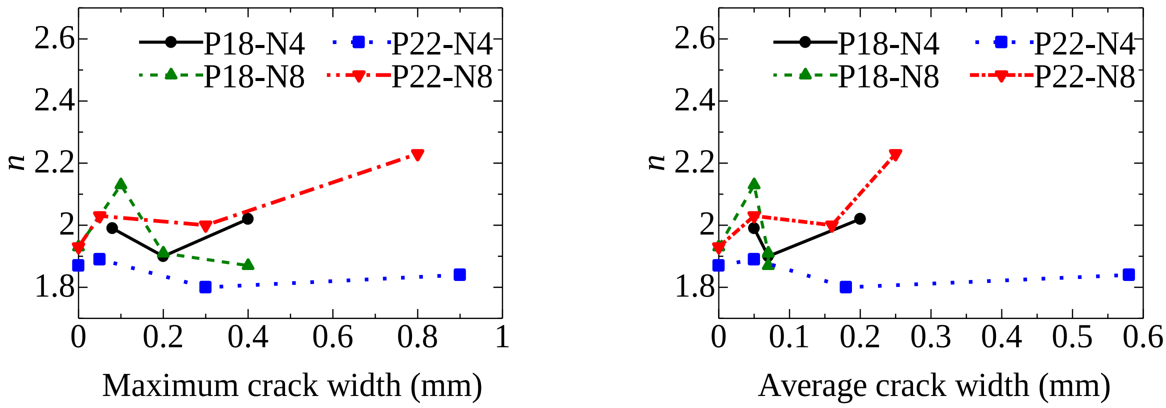

Fig. 11 Crack width before loading vs. *n*

Table 7 List of crack length ratio and calculated *n*

Specimen name	*n* Test results	Crack length ratio	Calculated *n*	Error (%)	Crack length ratio (0.3mm over)	Calculated *n*	Error (%)
P18-N4-T15	1.99	2	2.07	4	0	1.81	9
P18-N4-T65	1.90	4	2.33	23	0	1.81	5
P18-N4-T300	2.02	6	2.59	28	1	1.94	4
P18-N8-NF	1.93	0	1.81	6	0	1.81	6
P18-N8-T15	2.13	2	2.07	3	0	1.81	15
P18-N8-T65	1.91	8	2.85	50	0	1.81	5
P18-N8-T300	1.87	7	2.72	46	0	1.81	3
P22-N4-NF	1.87	0	1.81	3	0	1.81	3
P22-N4-T15	1.89	-	-	-	0	1.81	4
P22-N4-T65	1.80	6	2.59	44	2	2.07	15
P22-N4-T300	1.84	6	2.59	41	4	2.33	27
P22-N8-NF	1.93	0	1.81	6	0	1.81	6
P22-N8-T15	2.03	5	2.46	21	0	1.81	11
P22-N8-T65	2.00	10	3.11	56	2	2.07	4
P22-N8-T300	2.23	12	3.37	51	6	2.59	16

5. CONCLUSIONS

In this study, the uniaxial compressive test was conducted using RC columns specimens with induced corrosion cracks by aluminum pipe filled with expansion agent and the influence of cover concrete cracks due to bar corrosion on the compressive performance of RC columns was evaluated. The larger elapsed time after filling the expansion agent tends to increase the maximum crack width and average crack width. There is no significant relationship between induced cracks formulation and maximum stress obtained by compression test. The softening gradient of concrete has also no influence by the crack width before loading, the number of cracks, and crack length. Experimental results expressing the softening gradient of concrete show good agreements with calculated value, when induced cracks of equal or more than 0.3mm wide are considered.

REFERENCES

Mogawa, T., Kanakubo, T., Yasojima, A., Oyado, M. (2016), “Uniaxial Compressive Performance of RC Columns with Simulated Cracks due to Corrosion”, *Int. C. Asian Concrete Fed.*, Paper No. **44**

Mogawa, T., Kanakubo, T., Yasojima, A., Oyado, M. (2017), “Uniaxial Compressive Performance of RC Columns with Simulated Cracks due to Corrosion”, *Proceedings of the Japan Concrete Institute*, Vol. 39, No.**2,** 140-150 (in Japanese)

Syll, A. S., Kawamura, Y., Kanakubo, T. (2018), “Simulation of Concrete Cracks due to Bar corrosion by Aluminum Pipe Filled with An Expansion Agent”, *Summaries of Technical Papers of Annual Meeting, AIJ*, Structure IV, 55-56

Kawamura, Y., Kanakubo, T. (2018), “Flexural Performance of RC Beams with Simulated Cracks due to Bar Corrosion by Aluminum Pipe Filled with An Expansion Agent”, *Conference of Kanto Branch of JSCE*, V-22 (in Japanese)

Popovics, S. (1973), “A Numerical Approach to the Complete Stress-Strain Curve of Concrete”, *Cement Concrete Research*, Vol.**3**, 583-599